

# Defining regional infusion treatment strategies for extremity melanoma: comparative analysis of melphalan and temozolomide as regional chemotherapeutic agents

Yasunori Yoshimoto,<sup>1</sup> Christina K. Augustine,<sup>1</sup> Jin S. Yoo,<sup>1</sup> Patricia A. Zipfel,<sup>1</sup> M. Angelica Selim,<sup>2</sup> Scott K. Pruitt,<sup>1</sup> Henry S. Friedman,<sup>1</sup> Francis Ali-Osman,<sup>1</sup> and Douglas S. Tyler<sup>1</sup>

Departments of <sup>1</sup>Surgery and <sup>2</sup>Pathology, Duke University Medical Center, Durham, North Carolina

## Abstract

Five different human melanoma xenografts were used in a xenograft model of extremity melanoma to evaluate the variability of tumor response to regionally administered melphalan or temozolomide and to determine if various components of pertinent drug resistance pathways for melphalan [glutathione *S*-transferase (GST)/glutathione] and temozolomide [*O*<sup>6</sup>-alkylguanine DNA alkyltransferase (AGT)/mismatch repair (MMR)] could be predictive of tumor response. Xenograft-bearing rats underwent regional isolated limb infusion with either melphalan (90 mg/kg) or temozolomide (2,000 mg/kg). The levels of AGT activity, GST activity, glutathione level, and GST/AGT expression were examined in this group of xenografts and found to be quite heterogeneous. No correlation was identified between melphalan sensitivity and the GST/glutathione cellular detoxification pathway. In contrast, a strong correlation between the levels of AGT activity and percentage increase in tumor volume on day 30 ( $r = 0.88$ ) was noted for tumors treated with temozolomide. Regional therapy with temozolomide was more effective when compared with melphalan for the xenograft with the lowest AGT activity, whereas melphalan was more effective than temozolomide in another xenograft that had the highest AGT activity. In three other xenografts, there was no significant difference in response between the two chemotherapy agents. This study shows that AGT activity may be useful in predicting the utility of

temozolomide-based regional therapy for advanced extremity melanoma tumors. Our observations also point out the limited ability of analysis of the GST/glutathione pathway to predict response to chemotherapies like melphalan whose resistance is primarily mediated through a complex mechanism of detoxification. [Mol Cancer Ther 2007;6(5):1492–500]

## Introduction

Regional therapy in the form of either isolated limb perfusion or isolated limb infusion (ILI) has become an increasingly favored treatment for melanoma patients with intransit disease that is not amenable to simple surgical excision (1, 2). Regional therapy can yield drug concentrations ~10-fold higher than those achieved in systemic therapy while minimizing toxicity. Whereas significant durable responses are rarely seen with systemic therapy, regional therapy can achieve durable responses in 25% to 40% of melanoma patients as well as prolong the disease-free interval in the extremity over surgery alone (3, 4). The ability to achieve a complete response following isolated limb perfusion with melphalan is the strongest predictor of distant disease-free and overall survival (5, 6). Many patients, however, fail to respond completely to regional chemotherapy and some complete responders recur soon after their initial response. As such, there remains a great need to both expand regional therapy treatment options and develop better predictors of response within melanoma tumors. An ability to predict response will enable new treatments to be tailored to the patients most likely to respond to them.

Melphalan (also known as L-phenylalanine) is currently the drug of choice for use in both isolated limb perfusion and ILI. Failure to respond to melphalan regionally is largely due to the resistance mechanisms present in the tumor cell that center around the glutathione detoxification system (7). Temozolomide is a novel second-generation alkylating agent and an oral analogue of Dacarbazine (DTIC), which is currently Food and Drug Administration approved for the treatment of metastatic melanoma. Like DTIC, temozolomide is one of the most effective single agents in the treatment of systemic metastatic melanoma with relatively little toxicity (7). Temozolomide had equivalent antitumor activity compared with DTIC when tested head-to-head in a phase III randomized clinical trial in patients with stage IV melanoma and, although not currently U.S. Food and Drug Administration approved for stage IV melanoma patients, is frequently used off label to treat them due to its availability in an p.o. formulation (8). Both drugs work via the active metabolite 5-(3-methyltriazin-4-yl)imidazole-4-carboximide. However, unlike DTIC, which requires

Received 11/20/06; revised 2/13/07; accepted 3/23/07.

**Grant support:** Veterans Affairs Merit Review grant (D.S. Tyler), Institute of Genomic Sciences and Policy at Duke University Medical Center grant (D.S. Tyler, F. Ali-Osman, and H.S. Friedman), and American College of Surgeons Oncology Group Correlative Science grant (D.S. Tyler).

The costs of publication of this article were defrayed in part by the payment of page charges. This article must therefore be hereby marked *advertisement* in accordance with 18 U.S.C. Section 1734 solely to indicate this fact.

**Requests for reprints:** Douglas S. Tyler, Duke University Medical Center, Box 3118, Durham, NC 27710. Phone: 919-684-6858; Fax: 919-681-8701. E-mail: tyler002@acpub.duke.edu

Copyright © 2007 American Association for Cancer Research.

doi:10.1158/1535-7163.MCT-06-0718

metabolic dealkylation in the liver to form 5-(3-methyltriazenyl)imidazole-4-carboximide, temozolomide undergoes a chemical conversion to 5-(3-methyltriazenyl)imidazole-4-carboximide under physiologic conditions anywhere in the body (9). This difference is what makes temozolomide an attractive candidate for regional perfusion therapy. We have shown in a clinically relevant animal model of regionally advanced melanoma that regional temozolomide has significantly better antitumor activity than systemic temozolomide (10). Although temozolomide has not yet been approved for use as a regional chemotherapy agent in humans, an i.v. formulation of temozolomide has been developed and is currently undergoing testing for Food and Drug Administration approval. Resistance to temozolomide both systemically and regionally is largely due to one of two mechanisms: (a) high levels of  $O^6$ -alkylguanine DNA alkyltransferase (AGT) activity or (b) deficiency in the mismatch repair (MMR) pathway.

Given the availability of temozolomide as an alternate regional therapy agent in the near future and the distinctly different pathways associated with melphalan and temozolomide resistance, we sought to determine if tumors would respond differentially to these two chemotherapy agents. In addition, we examined the relationship between expression and activity of single molecular constituents of the melphalan and temozolomide resistance pathways in a panel of genetically unique melanomas to identify markers that could predict response to either agent. Specifically, we measured the expression and/or activity of several components of pathways associated with melphalan [glutathione *S*-transferase (GST)/glutathione] and temozolomide (AGT/MMR) resistance and compared this with the response observed to regional therapy. We hypothesized that by correlating specific chemoresistance pathways with response to regional therapy, we could identify markers that could predict the optimal chemotherapeutic agent for regional therapy of advanced melanoma. Such an approach would allow the development of mechanisms to identify optimal treatment strategies based on the underlying molecular characteristics of the tumor.

## Materials and Methods

### Tumor Cell Lines

Five human melanoma cell lines (DM6, DM366, DM440, DM443, and DM738) were selected to generate xenografts in our nude rat model (courtesy of Dr. Hilliard Seigler, Duke University, Durham, NC). Cells were maintained as a monolayer in Iscove's modified Dulbecco's medium with 10% fetal bovine serum, 2 mmol/L glutamine, 1,000 IU/mL penicillin, and 100 mg/mL streptomycin and grown at 37°C, 98% relative humidity, and 5% CO<sub>2</sub>.

### Animals and Tumor Inoculation

Female athymic nude rats (age, 5–7 weeks; weight, 95–120 g; RHU-M, Harlan or Charles River Laboratories International, Inc.) were housed with free access to food and water in a temperature-controlled room with a 12-h light-dark cycle. To facilitate tumor growth, rats were

subjected to 500 cGy of total body irradiation (Clinac 6X, Varian Medical Systems). Two days after irradiation, the rats were injected s.c. in the right distal hind limb with five million cultured human melanoma cells suspended in 0.15 mL of a 2:1 solution of PBS/Matrigel (Matrigel, BD Biosciences). Xenografts were measured every other day with Vernier calipers in two perpendicular dimensions. Tumor volume was calculated according to the following formula: (length × width<sup>2</sup>) / 2. All animal experimental protocols were approved by the Duke University and Durham Veterans Affairs Medical Center Institutional Animal Care and Use Committees.

### AGT Activity

AGT activity was measured as the removal of  $O^6$ -[<sup>3</sup>H]methylguanine from a [<sup>3</sup>H]-methylated DNA substrate as described previously (11). Briefly, xenograft tissue samples were homogenized, sonicated, and centrifuged for 30 min. For each sample, a known amount of protein was incubated in the reaction mixture at 37°C for 30 min. The DNA was precipitated by adding ice-cold perchloric acid (250 mmol/L), hydrolyzed by the addition of 0.1 N HCl and incubated at 70°C for 30 min. Following filtration with a microfilter apparatus, bases ( $N^7$  and  $O^6$ ) were separated by reverse-phase high-pressure liquid chromatography with 9% methanol in 0.5 mol/L ammonium formate. AGT activity was calculated as the amount of  $O^6$ -methylguanine released from the DNA substrate (femtomoles  $O^6$  lost) divided by the amount of sample protein added to the reaction mixture. Values are expressed as mean ± SE of at least three separate experiments. All experiments were done in parallel with negative control samples (heat-inactivated protein prepared from rat liver).

### GST Activity

GST activity was determined as described previously (12). All reagents were obtained from Sigma-Aldrich. Tissues were homogenized in 0.1 mol/L KPO<sub>4</sub> buffer with 1 mmol/L EDTA (pH 7.4) using a Beckman Polytron and lysed by two freeze/thaw cycles. Homogenates were centrifuged at 12,000 rpm for 30 min at 4°C. To determine total GST activity, supernatants were combined with 0.1 mol/L KPO<sub>4</sub> buffer (pH 6.5), 10 mmol/L chlorodinitrobenzene, and 10 mmol/L glutathione and the rate of conjugation of reduced glutathione to the substrate chlorodinitrobenzene was measured for 1 min at 340 nm in a Beckman spectrophotometer. Protein concentration was determined using the Bio-Rad protein assay (Bio-Rad). Assays were blanked with the reaction mix excluding supernatants. This mixture also served as a negative control.

### Glutathione Level

Total glutathione was determined as described previously (12, 13). All reagents were purchased from Sigma-Aldrich. Briefly, tumors were homogenized on ice in 10% sulfosalicylic acid (1:5 weight/volume) using a Brinkman Polytron (Brinkman Instruments Co.). Homogenates were centrifuged at 4,000 rpm for 5 min at 4°C. Supernatant (20 μL) was combined with 700 μL NADPH [0.3 mmol/L in glutathione assay buffer (NaPO<sub>4</sub>, pH 7.5, 6.3 mmol/L

EDTA)], 100  $\mu$ L DTNB (6 mmol/L in glutathione assay buffer), 170  $\mu$ L glutathione assay buffer, and 10  $\mu$ L glutathione reductase (55 units/mL in glutathione assay buffer), and the rate of reduction of DTNB was measured in a Beckman spectrophotometer at 412 nm for 1 min at 30°C. Total glutathione was calculated from a standard curve of the rate of reduction of DTNB in the presence of known amounts of glutathione. Assay components lacking sample supernatant served as the negative control. Glutathione levels are reported as nanomoles per milligram wet weight.

#### Quantitative PCR Method for GSTP1, GSTM1, GSTM3, GSTA1, and AGT

GSTP1, GSTM1, GSTA1, and AGT gene expression levels were measured using SYBR Green Real-time PCR methodology. Total RNA was isolated from tumor samples using the Qiagen RNeasy Mini kit. First-strand cDNA synthesis was carried out using the Roche Transcriptor First-Strand cDNA Synthesis kit. Quantitative PCR and data analysis were done using ABI SYBR Green Master Mix and an ABI 7900 Sequence Detector System. The primer sequences for  $\beta$ -actin were 5'-AGAAGCTGTGCTACGTCGC-3' and 5'-CGTCAGGCAGCTCGTAGCT-3'. The primer sequences for GSTP1 were 5'-TGCTGGACTTGCTGCTGATC-3' and 5'-CACATATGCTGAGAGCAG-3'. The primer sequences for GSTM1 were 5'-AGCACCATGCCATGATACT-3' and 5'-ACTGGCTTCTGTCATAATCA-3'. The primer sequences for GSTM3 were 5'-TCCGCACACAAGTATAAG-3' and 5'-CATGGAGAATTGTTTCAGTTG-3'. The primer sequences for GSTA1 were 5'-TCCAGCAAGTGCCAATG-3' and 5'-GCTGGCAATGTAGTTGAGA-3'. The primer sequences for AGT were 5'-ACAGAGTGGTCTGCAGCA-3' and 5'-ATCCTACTGCCACATACTCAG-3'. Expression values, normalized to  $\beta$ -actin, are expressed as mean of at least three separate experiments.

#### Assay for Microsatellite Instability

MMR status of our melanoma xenografts was determined by assessing microsatellite instability (MSI). Multiplex PCR was carried out with genomic DNA (14) to determine allelic size alterations as a measure of MSI using five mononucleotide markers: BAT25, BAT26, NR21, NR22, and NR24. The PCR products were then separated by capillary electrophoresis using ABI Prism 3100 Genetic Analyzer (Applied Biosystems), and the data were analyzed with GeneScan Analysis software to determine the size of the PCR products. MSI in more than two markers was defined as MSI, or MMR deficient, and MSI in two markers or less were considered MMR proficient (15).

#### Drugs for Xenograft Therapeutic Studies

The i.v. formulation of temozolomide was kindly provided by Schering Plough Research Institute. Melphalan was purchased from Glaxo Wellcome, Inc. A 4 mg/mL stock solution of temozolomide was prepared in PBS with 10% DMSO. A 0.2 mg/mL stock solution of melphalan was prepared in 0.9% sodium chloride. Stock solutions of drugs were routinely prepared immediately before surgery on the day of operation. The ILI infusate was prepared by further dilution of temozolomide stock solution with a 10% DMSO solution to achieve a final

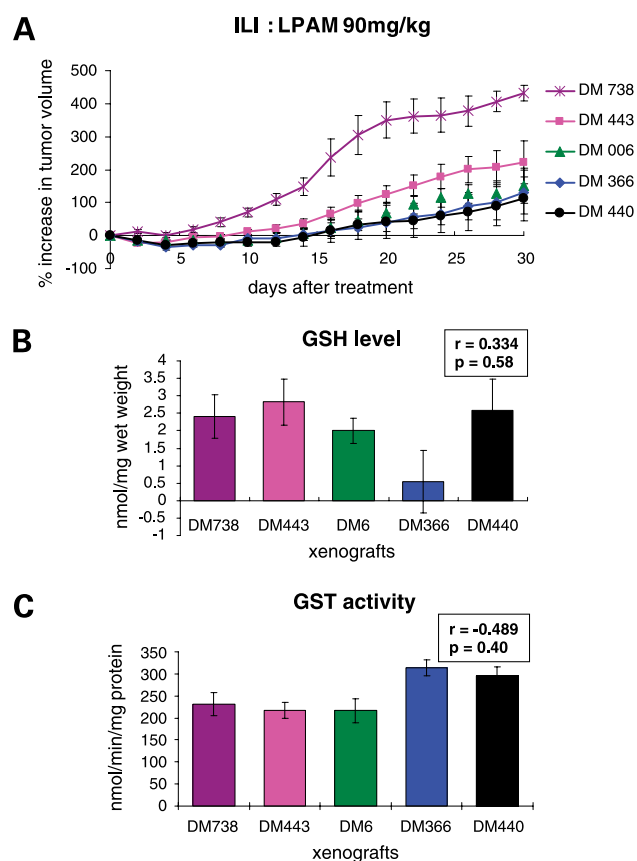


**Figure 1.** Molecular markers of resistance to melphalan (LPAM). **A**, percentage increase in tumor volume as a function of time following ILI using melphalan. *Y-axis*, percentage increase in tumor volume; *X-axis*, days after treatment. Each xenograft is an average of six rats. *Points*, mean; *bars*, SE. Measurements of molecular markers in xenografts. **B**, glutathione levels. **C**, GST activity. *Columns*, average of three independent determinations done in duplicate; *bars*, SE.

infusate concentration of 2,000 mg/kg in a volume of 22.5 mL. Likewise, the melphalan stock solution was further diluted with a 0.9% sodium chloride solution to achieve a final infusate concentration of 90 mg/kg in a volume of 22.5 mL.

#### Xenograft Therapy

Once tumor volume reached 1.2 to 1.6 cm<sup>3</sup> (~3–4 weeks following tumor inoculation), 18 rats were randomly assigned to each treatment group: (a) saline ILI, (b) temozolomide (2,000 mg/kg) ILI, or (c) melphalan (90 mg/kg) ILI. The drug doses of temozolomide and melphalan have been determined previously to be the maximum tolerated dose in this animal model producing an amputation rate of ~2% (16–18). In this study, only 1 of the 96 animals initially used lost an extremity secondary to the toxicity of the ILI treatment. This occurred shortly after the ILI procedure and another animal was added to this treatment group so that all groups would have six animals for tumor response outcome measures.

**Table 1. Growth characteristics of various melanoma xenografts treated with regional LPAM (90 mg/kg) and toxicity**

Xenograft	% Increase in tumor volume on day 30 (%; mean $\pm$ SE)	Quintupling time (d, mean $\pm$ SE)	Growth delay (d)	Regression no. of rats	Response CR/PR no. of rats	% Maximal decrease in tumor size (%; mean $\pm$ SE)
DM440	112.0 $\pm$ 66.9	50.1 $\pm$ 3.7	31.1	6/6	0/2	41.3 $\pm$ 12
DM443	222.7 $\pm$ 64.7	48.0 $\pm$ 5.4	24.2	4/6	1/1	45.5 $\pm$ 13.1
DM366	131.4 $\pm$ 65.8	46.2 $\pm$ 4.6	28.7	6/6	1/2	51.8 $\pm$ 11
DM6	150.7 $\pm$ 52.7	48.2 $\pm$ 5.4	28.5	4/6	0/1	30.8 $\pm$ 6.2
DM738	432.0 $\pm$ 24.4	23.2 $\pm$ 2.8	2.2	1/6	0/0	-0.7 $\pm$ 7.2

Abbreviations: CR, complete response; PR, partial response.

### ILI Technique

ILI was done as described previously (16–18) at room temperature. Under anesthesia, the right femoral artery and vein were isolated using an operating microscope through a 3-cm inguinal incision. The femoral artery was cannulated with a 24-gauge catheter and the arterial catheter was attached to a peristaltic pump (Master Flex model 7524-00, Cole-Parmer Instrument Co.). The femoral vein was then cannulated, and venous drainage flowed by gravity into the reservoir. Once both cannulas were in place, the thigh tourniquet was tightened, and saline was initiated at a flow rate of 1.5 mL/min by a peristaltic pump. A 15-min infusion with either melphalan or temozolomide was done at a flow rate of 1.5 mL/min followed by a 1-min washout infusion with saline at a flow rate of 3.0 mL/min. Following the wash, the tourniquet was loosened, and the distal femoral arterial and vein were ligated after removing the cannulas. Immediately after the surgery, animals received 2 mL saline s.c. as well as 3 mg gentamicin.

### Tumor Measurement and End Point

Tumors and any ulcer or full-thickness eschar were measured as described above. Tumor volume was calculated according to the same formula described above and the volume of any ulcer or eschar was subtracted from the overall tumor volume to estimate viable tumor volume. The response to treatment was followed until either a 500% change in tumor volume was achieved or 60 days had elapsed.

### Evaluation of Tumor Response and Toxicity

The response of the xenograft to the treatment was evaluated by the percentage increase in tumor volume

on day 30 after treatment, tumor quintupling time, maximal decrease in tumor volume, number of tumor regressions, and response to treatment for six animals per group.

The percentage increase in tumor volume was defined as the relative tumor volume on day 30 normalized to the initial tumor volume on the day of treatment (day 0). If, on any day after operation, tumor volume exceeded five times the volume measured on the day 0, data were censored at the date of last follow-up. Tumor quintupling time was defined as the mean number of days taken for individual tumors to reach a volume of five times their untreated volume on day 0. The maximal decrease in tumor volume was defined as the average percentage change in tumor volume on the day of the smallest volume after treatment. Tumor regressions were defined as a tumor whose overall volume decreased over two consecutive measurements. A complete response was defined as the disappearance of all measurable disease over at least two consecutive measurements and a partial response as a 50% or greater decrease in total tumor size over at least two consecutive measurements at any time during the follow-up period. Rats were also monitored for general well-being and functional ability of the treatment leg following surgery to access the toxicity.

### Statistical Analysis

The tumor response to chemotherapy was assessed by ANOVA. When significant differences were detected in ANOVA, differences between means were checked by Bonferroni's method. Fischer's exact test was done for

**Table 2. Growth characteristics of various melanoma xenografts treated with regional TMZ (2,000 mg/kg) and toxicity**

Xenograft	% Increase in tumor volume on day 30 (%; mean $\pm$ SE)	Quintupling time (d, mean $\pm$ SE)	Growth delay (d)	Regression no. of rats	Response CR/PR no. of rats	% Maximal decrease in tumor size (%; mean $\pm$ SE)
DM440	-23.62 $\pm$ 11.0	60.0 $\pm$ 0	41	6/6	0/6	79.9 $\pm$ 2.4
DM443	367.6 $\pm$ 39.7	30.1 $\pm$ 2.4	6.3	0/6	0/1	11.7 $\pm$ 12
DM366	115.1 $\pm$ 46.4	54.9 $\pm$ 3.1	37.4	6/6	2/2	66.7 $\pm$ 15
DM6	125.1 $\pm$ 87.3	47.3 $\pm$ 5.1	27.6	6/6	2/0	48 $\pm$ 17
DM738	-27.22 $\pm$ 30.1	51.6 $\pm$ 4.3	30.6	6/6	3/3	91.6 $\pm$ 4.7

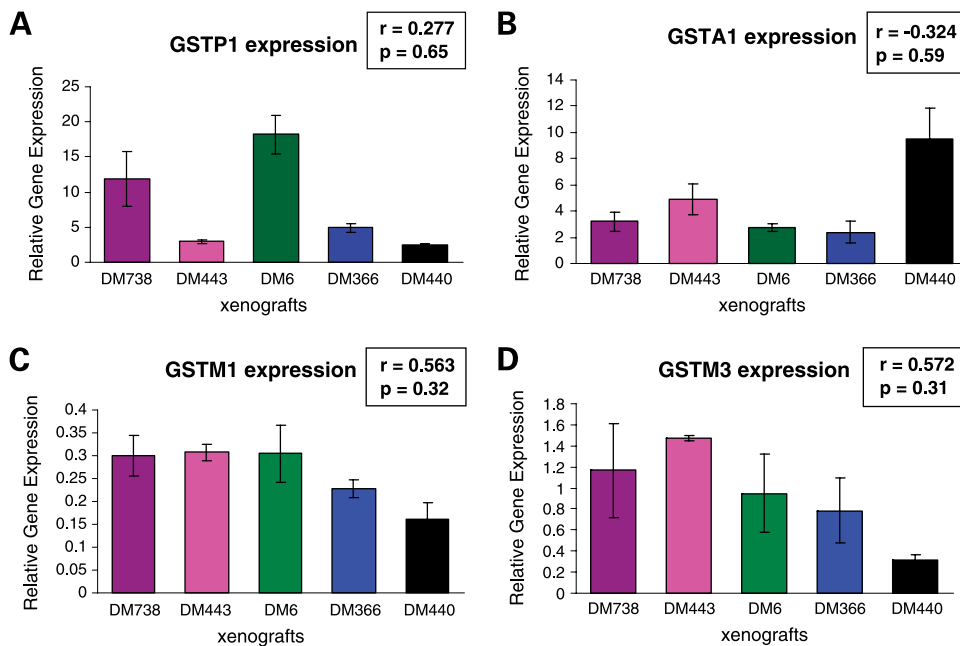


**Figure 2.** GST expression and resistance to melphalan. GST expression in xenografts. **A**, GSTP1. **B**, GSTA1. **C**, GSTM1. **D**, GSTM3. Y-axis, relative gene expression. Correlation between percentage increase in tumor volume on day 30 using melphalan and GST expression is also shown with the respective figures.

tumor regressions.  $P$  values  $<0.05$  were considered significant. Correlation coefficient was obtained using simple regression analysis.

## Results

### Molecular Markers of Resistance to Melphalan

We evaluated the spectrum of sensitivity to melphalan in a series of five human melanoma xenografts (see Table 1). In Fig. 1A, the percentage change in tumor volume is plotted as a function of time following ILI using melphalan for each xenograft (DM366, DM440, DM443, DM6, and DM738). Each line is an average of six rats (error bars indicate SE). There were statistically significant differences in sensitivity across this panel of xenografts with DM738 being the most resistant and DM440 the most susceptible to melphalan ( $P = 0.05$ ).

We then tested several molecular constituents of the glutathione detoxification pathway to identify markers that might correlate with sensitivity to melphalan. Glutathione levels across this panel of xenografts were heterogeneous ranging from 0.54 nmol/mg for xenograft DM366 to 2.82 nmol/mg for xenograft DM443 (Fig. 1B) and showed no correlation with melphalan sensitivity [ $r = 0.33$ ;  $P =$  not significant (NS)]. In contrast to glutathione, the level of total GST activity across our panel of five human melanoma xenografts varied little, as shown in Fig. 1C, ranging from 216 nmol/min/mg protein (DM6) to 314 nmol/min/mg protein (DM366). Like glutathione, GST activity showed no correlation with sensitivity to melphalan ( $r = -0.49$ ;  $P =$  NS).

Total GST activity, however, reflects the sum of the activity of at least eight different GST isoforms with multiple subtypes, the most prevalent being GSTP1, GSTM1, GSTM3, and GSTA1. To evaluate the correlation of these particular

GST isoform to melphalan sensitivity, we quantified the RNA expression for each isoform using quantitative PCR. These results are summarized in Fig. 2. Analysis of GSTP1 expression revealed marked differences in expression across this panel of xenografts ( $P < 0.001$ ) ranging from 2.44 for DM440 to 19.1 for DM6 (Fig. 2A). There was no correlation between GSTP1 expression and melphalan sensitivity as measured by percentage increase in tumor volume on day 30 after treatment ( $r = 0.28$ ;  $P =$  NS). Additional measures of tumor response following ILI with melphalan including tumor quintupling time and tumor growth delay showed no correlation with GSTP1 expression levels. GSTA1 expression levels also varied significantly across this panel of xenografts ( $P = 0.025$ ) ranging from 2.39 for DM366 to 9.5 for DM440 (Fig. 2B) and likewise showed no correlation with melphalan sensitivity as measured by percentage increase in tumor volume by day 30 ( $r = -0.32$ ;  $P =$  NS), tumor quintupling time ( $r = -0.36$ ;  $P =$  NS), or tumor growth delay ( $r = 0.22$ ;  $P =$  NS) following ILI with melphalan. The expression level of GSTM1 and GSTM3 varied little across this panel of xenografts (Fig. 2C and D) and showed no correlation with melphalan sensitivity ( $r = 0.56$ ,  $P =$  NS;  $r = 0.57$ ,  $P =$  NS, respectively).

### Molecular Markers of Resistance to Temozolomide

We used the same panel of five human melanoma xenografts to evaluate the spectrum of sensitivity to regionally administered temozolomide (see Table 2). There were marked differences in sensitivity across this panel of xenografts ( $P < 0.0001$ ), as shown in Fig. 3A where percentage change in tumor volume is plotted as a function of time following ILI with the i.v. formulation of temozolomide. Each line represents one xenograft (DM6, DM738, DM443, DM440, or DM366) and is the average of six rats (error bars depict SE). Xenografts DM738 and DM440, with

percentage tumor increases of only  $-27.22$  and  $-23.62$ , respectively, on day 30, were significantly more sensitive to temozolomide than DM443, with a percentage tumor increase on day 30 of  $367.6$  ( $P = 0.002$  and  $0.002$ , respectively).

We hypothesized that the differential sensitivity to temozolomide observed in our panel of xenografts could be correlated with the efficacy of the temozolomide resistance mechanisms of the tumor. Although deficiency in the MMR pathway is uncommon in melanoma, we evaluated the importance of this pathway in our panel of xenografts. We assessed MMR status by measuring the degree of MSI using five mononucleotide markers (BAT-25, BAT-26, NR-21, NR-22, and NR-25). No MSI was detected (data not shown), suggesting that the MMR pathway is intact in these xenografts and thus not a likely contributor to temozolomide resistance in our system.

To evaluate the contribution of the AGT pathway to temozolomide resistance, we measured both AGT activity and expression in each xenograft. As shown in Fig. 3B, the level of AGT activity across this panel of xenografts was quite heterogeneous ranging from  $31.14$  fmoles/mg protein for xenograft DM738 up to  $319.3$  fmoles/mg protein for xenograft DM6. We observed a strong correlation between the levels of AGT activity and percentage increase in tumor volume on day 30 ( $r = 0.88$ ;  $P = 0.1$ ), clearly illustrating the relationship between AGT activity and tumor response to regional temozolomide. Xenografts with low AGT activity (e.g., DM738 and DM440) showed much higher levels of response to regional temozolomide than xenografts with high AGT activity (e.g., DM443). Additional measures of tumor response following ILI with regional temozolomide, as shown in Table 2, likewise showed strong correlations with AGT activity and include tumor quintupling time ( $r = -0.67$ ;  $P = 0.21$ ) and maximal decrease in tumor volume ( $r = -0.98$ ;  $P \leq 0.005$ ). A heterogeneous pattern was also seen across this panel of xenografts for AGT expression (Fig. 3C); however, a similar correlation was not observed between tumor response to temozolomide and RNA expression level of AGT ( $r = 0.48$ ;  $P = \text{NS}$ ).

### Differential Response of Melanoma Tumors to Regional Chemotherapeutic Agents

Although we were unable to identify a single marker predictive of tumor response to melphalan treatment, there were marked differences in how tumors responded to melphalan and temozolomide. For each melanoma xenograft, mean quintupling time after treatment with either melphalan (blue columns) or temozolomide (red columns) at equitoxic dosages (90 and 2,000 mg/kg, respectively) is shown in Fig. 4. Also shown is the mean quintupling time for tumors treated with a control saline infusion. The marked differential response of each xenograft to these two different chemotherapies can be clearly seen. The number of days between tumor inoculation and ILI operation were not significantly different among any of the xenografts (average,  $25.7 \pm 1.1$  days; mean value  $\pm$  SE). Likewise, neither initial tumor volume on day 0 nor preoperation body weight ( $1.48 \pm 0.09$  cm<sup>3</sup> and  $152 \pm 6.5$  g, respectively) varied

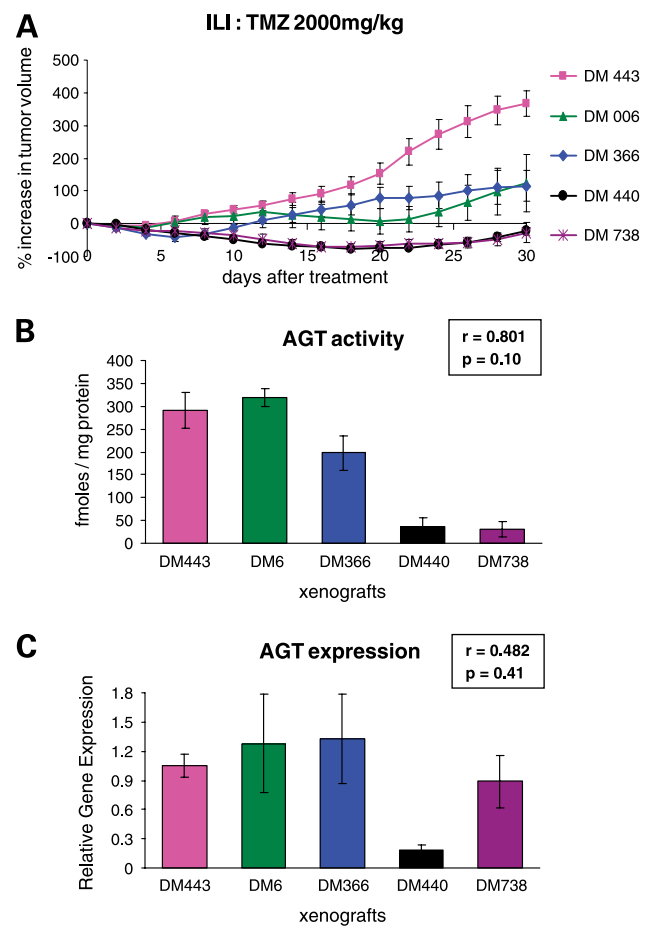


**Figure 3.** Molecular markers of resistance to temozolomide. **A**, percentage increase in tumor volume as a function of time following ILI using temozolomide (TMZ). Y-axis, percentage increase in tumor volume on day 30; X-axis, days after treatment. Each xenograft is an average of six rats. Points, mean; bars, SE. AGT activity (**B**) and AGT expression (**C**) in the xenografts. Correlation between percentage increase in tumor volume on day 30 using temozolomide and AGT activity and AGT expression is shown with the figures.

significantly among any of the xenograft groups. The tumor quintupling time after regional temozolomide or melphalan treatment, however, varied significantly for xenografts DM738 and DM443 ( $P < 0.001$  and  $P < 0.015$ , respectively), with xenograft DM738 being significantly more sensitive to temozolomide and xenograft DM443 being significantly more sensitive to melphalan. The three remaining xenografts (DM440, DM6, and DM366) showed a more uniform response to the two chemotherapy agents that, while slightly favoring temozolomide, was not statistically different with regard to tumor quintupling time.

### Discussion

In this study, we used a clinically relevant xenograft model of extremity melanoma to assess the relationship between the *in vivo* antitumor activity of two chemotherapy reagents

(melphalan and temozolomide) and the expression level/activity of molecular constituents of pathways known to confer resistance to these drugs. This relationship was examined across five human melanoma xenografts, each with markedly different patterns of resistance activity. We identified a molecular marker that correlated with temozolomide responsiveness; however, we could not find a marker that correlated with sensitivity to melphalan. The demonstration of a direct correlation between resistance to temozolomide and the levels of AGT activity in the tumor and, further, that sensitivity to temozolomide in the setting of regional infusion therapy for melanoma can be predicted by the levels of AGT activity are novel and have important clinical implications. Our model, with its ability to test several human melanoma xenografts, is the first report to clearly show the relationship between AGT activity and resistance to temozolomide in an *in vivo* setting. Previous studies have looked at temozolomide efficacy following modulation of AGT activity; however, these experiments were done only in an *in vitro* setting (15, 19).

Our results showing the strong correlation between AGT activity and temozolomide resistance are consistent with other studies that implicate AGT as one of the key enzymes regulating resistance to alkylating agents (15, 20, 21). AGT repairs DNA methyl adducts by transferring the methyl adduct at the  $O^6$  position of guanine to an internal cysteine residue in an autoinactivating reaction. Although more than 14 different alkylation sites on DNA have been

described, those at the  $O^6$  position are the most cytotoxic and are ultimately responsible for the therapeutic effects observed clinically. The theory that depletion of AGT by the competitive inhibitor  $O^6$ -benzylguanine ( $O^6$ BG) can enhance the antitumor activity of alkylating agents has been well shown experimentally (20, 21), and studies are under way to evaluate the utility of such agents in a clinical setting (22–24).

Despite its therapeutic advantages, however, systemically administered  $O^6$ BG has the potential for dose-related acute toxicity to the hematopoietic system when used in combination therapies with systemically administered chemotherapeutic agents. In a phase II trial of  $O^6$ BG plus an alkylating agent, grade 3 to 4 myelosuppression was observed in 57% of patients, with no improvement in the clinical outcome (23). In the regional chemotherapy setting, systemic toxicity can be minimized, as only the modulator  $O^6$ BG would be given systemically. We have shown previously the effectiveness of this strategy in our xenograft model using DM6 melanoma, where responses to regional temozolomide were markedly improved with the concurrent administration of systemic  $O^6$ BG in the absence of any increased toxicity (25).

It remains to be determined if tumors with low AGT activity, which respond well to temozolomide alone, will respond further to modulation with  $O^6$ BG. *In vitro* data suggest that cell lines with low or undetectable levels of AGT activity are quite sensitive to temozolomide alone and

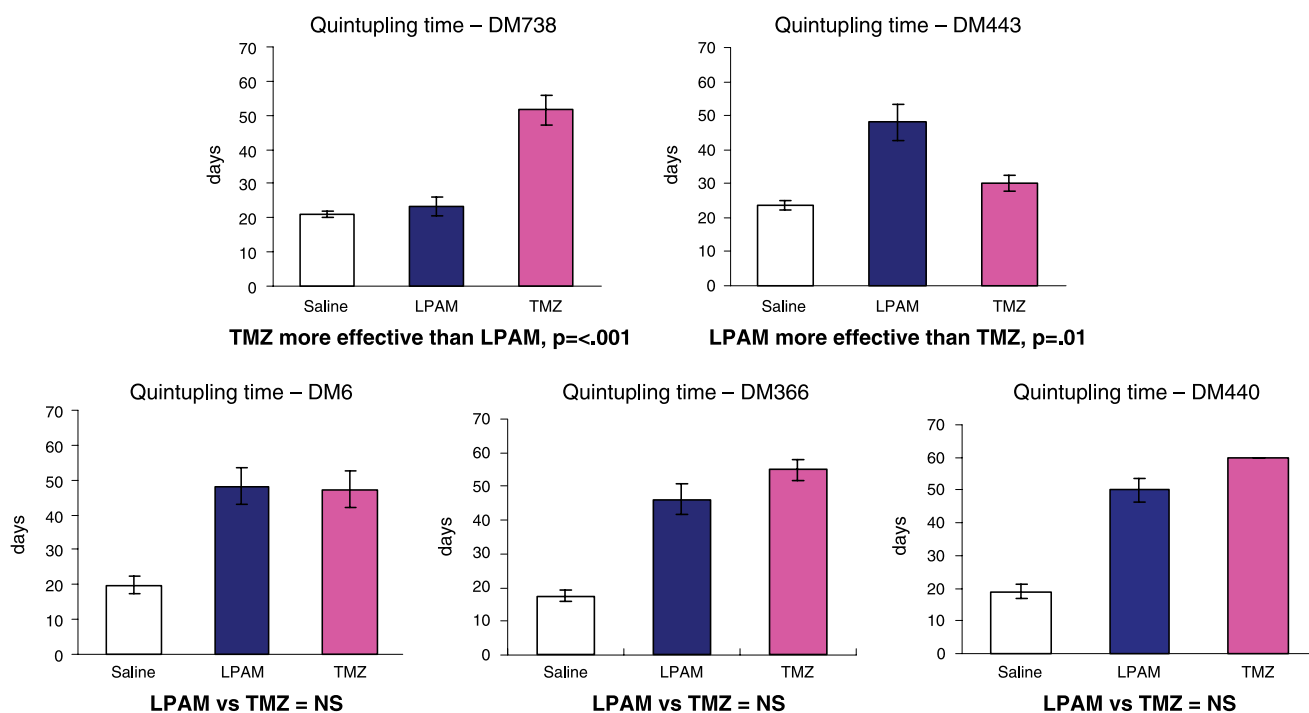


**Figure 4.** Temozolomide (2,000 mg/kg) versus melphalan (90 mg/kg). Y-axis, tumor quintupling time (days); X-axis, tumor treatment for each of the five melanoma xenografts tested. Three treatment groups are shown for each xenograft: (a) saline ILI, (b) temozolomide (2,000 mg/kg) ILI, or (c) melphalan (90 mg/kg) ILI. Each treatment group within a specific xenograft has an average of six rats. Columns, mean; bars, SE. The P values are for analyzing the significance of the difference in tumor growth between melphalan and temozolomide treatment.

do not show increased chemosensitivity with O<sup>6</sup>BG treatment (15). As such, determination of AGT activity would also have potential utility in a clinical setting to help identify patients most likely to benefit from AGT modulation therapy as opposed to those who could be treated with chemotherapy alone.

Other mechanisms known to confer resistance to temozolomide include deficiency in the MMR pathway and activity of the base excision repair system. Although AGT protects cells against the cytotoxic effects of methylating agents, cell death in response to methylating agents actually occurs as a consequence of the MMR pathway, whereby unrepaired O<sup>6</sup>MG residues pair with thymines during replication triggering a futile cycle of the MMR pathway and ultimately cell death. However, as deficiency in the MMR pathway occurs infrequently in melanoma (26), it is unlikely to contribute to temozolomide resistance in our system. A recent report implicated the base excision repair pathway as a major contributor to cellular resistance to temozolomide showing that temozolomide efficacy is dependent on expression and activity of specific base excision repair genes (27). Previous reports have also suggested that base excision repair and nucleotide excision repair may contribute to drug resistance but their respective roles in the prevention of mutations are not clear (28).

GSTs are a polygenic group of enzymes involved in detoxification of a wide range of xenobiotics and chemotherapeutic agents. GSTs catalyze the conjugation of reactive electrophiles to the tripeptide glutathione, thereby inactivating the electrophile. Overexpression of GSTs is thought to be a significant mechanism by which human tumor cells become resistant to the cytotoxic effects of alkylating agents. Recent studies have shown that various tumors express elevated levels of glutathione. Moreover, there is evidence suggesting that glutathione plays a crucial role in cell proliferation and tumor resistance (29). We have shown previously a strong correlation between *in vitro* melphalan sensitivity, glutathione level, and GST activity (12). We also observed a direct correlation between the duration of melphalan exposure and the level of glutathione in residual melanoma xenografts (30), suggesting that tumor cells able to survive treatment with melphalan have higher glutathione levels, thereby enhancing their ability to inactivate the drug. Furthermore, we could show marked improvements in melanoma tumor responses to melphalan regional therapy by pretreating animals with buthionine sulfoximine to deplete glutathione and decrease GST activity (30). Despite this, we could not show a clear relationship between glutathione level, GST activity or expression, and sensitivity to melphalan *in vivo* underscoring the complexity of the GST/glutathione resistance pathway. It is this complexity that may limit the utility of a single molecular marker as a predictor of sensitivity to melphalan. Rather, multiple molecular markers or a larger scale gene expression profile may be more useful predictors of sensitivity to melphalan.

Further complicating this issue is that at least eight different types of human GSTs have been identified:  $\alpha$ ,  $\mu$ ,  $\pi$ ,

$\sigma$ ,  $\theta$ ,  $\zeta$ ,  $\omega$ , and  $\kappa$  (31), and many previous studies have drawn conflicting conclusions about their role in chemoresistance. One study suggested that increased expression of GSTA1 is primarily responsible for acquired drug resistance (30), whereas other studies have suggested that GSTP1 and GSTM1 are responsible for drug resistance (32, 33). Horton et al. (34) showed a near-linear correlation between resistance to a bifunctional alkylating agent and overexpression of the  $\mu$  class of GSTs and suggested that overexpression of the GSTMs may be responsible for the observed resistance of ovarian carcinoma cells to bifunctional alkylating agents. Dulik et al. (35) reported an association between increased expression of GSTA1 in drug-resistant tumor cells and resistance to melphalan, whereas Paumi et al. (36) and Depeille et al. (33) showed no correlation between GSTM1 and sensitivity to melphalan in melanoma cell line. It is clear from these reports that identifying the GSTs important for drug resistance is not only complex but will likely be dependent on both the tumor type and the alkylating agent. Our data show that, at least in melanoma, the expression level of the  $\mu$  class of GSTs does not figure prominently in melphalan resistance. Further work is necessary to elucidate the relationship between GSTs expression and melphalan resistance. It has also been suggested that there is an association between AGT and GSTP1 (37) or a synergistic action between AGT and glutathione (19). Overall, we found no correlation between any of the biochemical variables of the GST detoxification and chemoresistance to temozolomide or melphalan in our experiments.

Melanomas show considerable heterogeneity in their sensitivity to alkylating agents despite their phenotypic similarities, making it difficult to predict optimal therapeutic strategies. Our findings show that in some cases, such as with temozolomide, the molecular properties of a tumor can be used to predict sensitivity of that tumor to chemotherapeutic agents. Unfortunately, measurements of AGT activity are relatively labor intense for incorporation into large-scale clinical trials. Furthermore, the complexity of some drug resistance mechanisms, such as the glutathione detoxification system for melphalan, precludes accurate characterization using a single marker. Although our *in vivo* tumor responses suggest that melanoma tumors may have intrinsically different susceptibilities to various chemotherapy agents, a more detailed analysis such as in the form of drug resistance gene profile signatures (38) might be required before an individualized treatment regimen can be developed for patients based on host genetic factors and inherent tumor biology.

#### Acknowledgments

We thank Rick Leary for care of animals, Spencer Bridges for assistance of xenograft experiments, and Rob Holzknicht for maintenance of cell lines.

#### References

1. Kremenz ET, Carter RD, Sutherland CM, et al. Regional chemotherapy for melanoma. A 35-year experience. *Ann Surg* 1994;220:520–34; discussion 34–5.
2. Hayes AJ, Clark MA, Harries M, Thomas JM. Management of in-transit



- metastases from cutaneous malignant melanoma. *Br J Surg* 2004;91:673–82.
3. Lindner P, Doubrovsky A, Kam PC, Thompson JF. Prognostic factors after isolated limb infusion with cytotoxic agents for melanoma. *Ann Surg Oncol* 2002;9:127–36.
  4. Noorda EM, Takkenberg B, Vrouwenraets BC, et al. Isolated limb perfusion prolongs the limb recurrence-free interval after several episodes of excisional surgery for locoregional recurrent melanoma. *Ann Surg Oncol* 2004;11:491–9.
  5. Aloia TA, Grubbs E, Onaitis M, et al. Predictors of outcome after hyperthermic isolated limb perfusion: role of tumor response. *Arch Surg* 2005;140:1115–20.
  6. Noorda EM, Vrouwenraets BC, Nieweg OE, et al. Isolated limb perfusion for unresectable melanoma of the extremities. *Arch Surg* 2004;139:1237–42.
  7. Newlands ES, Stevens MF, Wedge SR, Wheelhouse RT, Brock C. Temozolomide: a review of its discovery, chemical properties, pre-clinical development, and clinical trials. *Cancer Treat Rev* 1997;23:35–61.
  8. Middleton MR, Grobb JJ, Aaronson N, et al. Randomized phase III study of temozolomide versus decarbazine in the treatment of patients with advanced metastatic malignant melanoma. *J Clin Oncol* 2000;18:158–66.
  9. Horspool KR, Stevens MF, Newton CG, et al. Antitumor imidazotrazines. 20. Preparation of the 8-acid derivative of mitozolomide and its utility in the preparation of active antitumor agents. *J Med Chem* 1990;33:1393–9.
  10. Ueno T, Ko SH, Grubbs E, et al. Temozolomide is a novel regional infusion agent for the treatment of advanced extremity melanoma. *Am J Surg* 2004;188:532–7.
  11. Domoradzki J, Pegg AE, Dolan ME, Maher VM, McCormick JJ. Correlation between  $O^6$ -methylguanine-DNA-methyltransferase activity and resistance of human cells to the cytotoxic and mutagenic effect of *N*-methyl-*N'*-nitro-*N*-nitrosoguanidine. *Carcinogenesis* 1984;5:1641–7.
  12. Grubbs EG, Abdel-Wahab O, Cheng TY, et al. In-transit melanoma: the role of alkylating-agent resistance in regional therapy. *J Am Coll Surg* 2004;199:419–27.
  13. Grubbs EG, Ueno T, Abdel-Wahab O, et al. Modulation of resistance to regional chemotherapy in the extremity melanoma model. *Surgery* 2004;136:210–8.
  14. Suraweera N, Duval A, Reperant M, et al. Evaluation of tumor microsatellite instability using five quasimonomorphic mononucleotide repeats and pentaplex PCR. *Gastroenterology* 2002;123:1804–11.
  15. Pepponi R, Marra G, Fuggetta MP, et al. The effect of  $O^6$ -alkylguanine-DNA alkyltransferase and mismatch repair activities on the sensitivity of human melanoma cells to temozolomide, 1,3-bis(2-chloroethyl)-1-nitrosourea, and cisplatin. *J Pharmacol Exp Ther* 2003;304:661–8.
  16. Abdel-Wahab OI, Grubbs E, Viglianti BL, et al. The role of hyperthermia in regional alkylating agent chemotherapy. *Clin Cancer Res* 2004;10:5919–29.
  17. Ko SH, Ueno T, Yoshimoto Y, et al. Optimizing a novel regional chemotherapeutic agent against melanoma: hyperthermia-induced enhancement of temozolomide cytotoxicity. *Clin Cancer Res* 2006;12:289–97.
  18. Thompson JF, Lai DT, Ingvar C, Kam PC. Maximizing efficacy and minimizing toxicity in isolated limb perfusion for melanoma. *Melanoma Res* 1994;4 Suppl 1:45–50.
  19. Passagne I, Evrard A, Depeille P, et al.  $O(6)$ -Methylguanine DNA-methyltransferase (MGMT) overexpression in melanoma cells induces resistance to nitrosoureas and temozolomide but sensitizes to mitomycin C. *Toxicol Appl Pharmacol* 2006;211:97–105.
  20. Wedge SR, Porteous JK, Newlands ES. Effect of single and multiple administration of an  $O^6$ -benzylguanine/temozolomide combination: an evaluation in a human melanoma xenograft model. *Cancer Chemother Pharmacol* 1997;40:266–72.
  21. Kokkinakis DM, Bocangel DB, Schold SC, Moschel RC, Pegg AE. Thresholds of  $O^6$ -alkylguanine-DNA alkyltransferase which confer significant resistance of human glial tumor xenografts to treatment with 1,3-bis(2-chloroethyl)-1-nitrosourea or temozolomide. *Clin Cancer Res* 2001;7:421–8.
  22. Quinn JA, Desjardins A, Weingart J, et al. Phase I trial of temozolomide plus  $O^6$ -benzylguanine for patients with recurrent or progressive malignant glioma. *J Clin Oncol* 2005;23:7178–87.
  23. Gajewski TF, Sosman J, Gerson SL, et al. Phase II trial of the  $O^6$ -alkylguanine DNA alkyltransferase inhibitor  $O^6$ -benzylguanine and 1,3-bis(2-chloroethyl)-1-nitrosourea in advanced melanoma. *Clin Cancer Res* 2005;11:7861–5.
  24. Warren KE, Aikin AA, Libucha M, et al. Phase I study of  $O^6$ -benzylguanine and temozolomide administered daily for 5 days to pediatric patients with solid tumors. *J Clin Oncol* 2005;23:7646–53.
  25. Ueno T, Ko SH, Grubbs E, et al. Modulation of chemotherapy resistance in regional therapy: a novel therapeutic approach to advanced extremity melanoma using intra-arterial temozolomide in combination with systemic  $O^6$ -benzylguanine. *Mol Cancer Ther* 2006;5:732–8.
  26. Kohonen-Corish MR, Cooper WA, Saab J, et al. Promoter hypermethylation of the  $O(6)$ -methylguanine DNA methyltransferase gene and microsatellite instability in metastatic melanoma. *J Invest Dermatol* 2006;126:167–71.
  27. Trivedi RN, Almeida KH, Fornasaglio JL, Schamus S, Sobol RW. The role of base excision repair in the sensitivity and resistance to temozolomide-mediated cell death. *Cancer Res* 2005;65:6394–400.
  28. Aloyz R, Xu ZY, Bello V, et al. Regulation of cisplatin resistance and homologous recombinational repair by the TFIIF subunit XPD. *Cancer Res* 2002;62:5457–62.
  29. McClean S, Hill BT. An overview of membrane, cytosolic, and nuclear proteins associated with the expression of resistance to multiple drugs *in vitro*. *Biochim Biophys Acta* 1992;1114:107–27.
  30. Morrow CS, Smitherman PK, Diah SK, Schneider E, Townsend AJ. Coordinated action of glutathione *S*-transferases (GSTs) and multidrug resistance protein 1 (MRP1) in antineoplastic drug detoxification. Mechanism of GST A1-1 and MRP1-associated resistance to chlorambucil in MCF7 breast carcinoma cells. *J Biol Chem* 1998;273:20114–20.
  31. Procopio A, Alcaro S, Cundari S, et al. Molecular modeling, synthesis, and preliminary biological evaluation of glutathione-*S*-transferase inhibitors as potential therapeutic agents. *J Med Chem* 2005;48:6084–9.
  32. Harbottle A, Daly AK, Atherton K, Campbell FC. Role of glutathione *S*-transferase P1, P-glycoprotein, and multidrug resistance-associated protein 1 in acquired doxorubicin resistance. *Int J Cancer* 2001;92:777–83.
  33. Depeille P, Cuq P, Mary S, et al. Glutathione *S*-transferase M1 and multidrug resistance protein 1 act in synergy to protect melanoma cells from vincristine effects. *Mol Pharmacol* 2004;65:897–905.
  34. Horton JK, Roy G, Piper JT, et al. Characterization of a chlorambucil-resistant human ovarian carcinoma cell line overexpressing glutathione *S*-transferase  $\mu$ . *Biochem Pharmacol* 1999;58:693–702.
  35. Dulik DM, Fenselau C, Hilton J. Characterization of melphalan-glutathione adducts whose formation is catalyzed by glutathione transferases. *Biochem Pharmacol* 1986;35:3405–9.
  36. Paumi CM, Ledford BG, Smitherman PK, Townsend AJ, Morrow CS. Role of multidrug resistance protein 1 (MRP1) and glutathione *S*-transferase A1-1 in alkylating agent resistance. Kinetics of glutathione conjugate formation and efflux govern differential cellular sensitivity to chlorambucil versus melphalan toxicity. *J Biol Chem* 2001;276:7952–6.
  37. Gilliland FD, Harms HJ, Crowell RE, et al. Glutathione *S*-transferase P1 and NADPH quinone oxidoreductase polymorphisms are associated with aberrant promoter methylation of P16(INK4a) and  $O(6)$ -methylguanine-DNA methyltransferase in sputum. *Cancer Res* 2002;62:2248–52.
  38. Potti A, Dressman HK, Bild A, et al. Genomic signatures to guide the use of chemotherapeutics. *Nat Med* 2006;12:1294–300.